

Article

Analysis of Interannual Anomalies and Causes of Compound Extreme Wind and Precipitation Events in Spring over the Jiangsu–Anhui Region

Jing Zhou ¹, Yan Sun ^{1,*}, Lei Liu ² and Lingli Zhai ³¹ Jiangsu Provincial Institute of Meteorological Science, Nanjing 210019, China; gemini_zj@126.com² Wuhu Meteorological Bureau, Wuhu 241000, China³ Jiangsu Provincial Meteorological Information Center, Nanjing 210019, China

* Correspondence: jsshqxtsy@sina.com

Abstract: By using the daily average wind speed and precipitation data of 125 stations in Jiangsu and Anhui Provinces of China from 1961 to 2020 and the monthly NCEP/NCAR reanalysis data, the interannual variation characteristics and its possible reasons of spring compound extreme wind and precipitation events in the Jiangsu–Anhui region were discussed. Results show that the spring compound extreme wind and precipitation events generally present a lesser distribution in the south and more in the north. The events occurring in south (north) of 32° N are basically less than (above) three days, and in some areas of northern Jiangsu, it can reach more than four days. On a regional average, the spring compound extreme wind and precipitation events have presented a significant downward trend in the past 60 years. In addition, there was an interdecadal mutation from more to less in the early 1990s, with the most significant decline in the coastal areas of northern Jiangsu. Further analysis reveals that the synthetic height anomaly field at 500 hPa corresponding to the frequent occurrence of the spring compound extreme wind and precipitation events is positive in the northern region of 45° N, while it is negative in the southern region of 45° N, which enhances the high pressure in high latitudes, increases the meridional gradient of circulation, and promotes the activity of high-latitude short-wave trough ridges and cold air. Meanwhile, a strong southwest airflow exists in the corresponding middle and low latitudes at 850 hPa, so the water vapor from the Bay of Bengal can be continuously transported to the Jiangsu–Anhui region. Overall, the abundant water vapor transportation and the convergence of southward cold air in high latitudes are conducive to the occurrence of extreme wind and precipitation events.

Keywords: compound extreme wind and precipitation events; interannual anomaly; circulation background; Jiangsu–Anhui region



Citation: Zhou, J.; Sun, Y.; Liu, L.; Zhai, L. Analysis of Interannual Anomalies and Causes of Compound Extreme Wind and Precipitation Events in Spring over the Jiangsu–Anhui Region. *Atmosphere* **2023**, *14*, 1290. <https://doi.org/10.3390/atmos14081290>

Academic Editors: Chuhan Lu, Dachao Jin and Yan Bao

Received: 25 May 2023

Revised: 27 July 2023

Accepted: 5 August 2023

Published: 15 August 2023



Copyright: © 2023 by the authors. Licensee MDPI, Basel, Switzerland. This article is an open access article distributed under the terms and conditions of the Creative Commons Attribution (CC BY) license (<https://creativecommons.org/licenses/by/4.0/>).

1. Introduction

In the past few decades, extreme weather and climate events have been extensively studied and considerable progresses have been made. The Synthesis Report of the Sixth Assessment Report of IPCC (hereinafter referred to as IPCC AR6) [1] points out that, in the context of global warming, the frequency, amplitude, and intensity of heavy precipitation in the future are positively correlated with the magnitude of global warming. Simulation analysis shows that with the increase in global warming, the frequency and amplitude of heavy precipitation events increase acceleratingly. In the future, for every 1 °C increase in global temperature, the intensity of extreme daily precipitation events will increase by 7% (passing high reliability test). The more extreme the heavy precipitation event, the greater the frequency amplitude (passing high reliability test).

Meanwhile, researchers pointed out that, since the mid-20th century, the wind speed in middle- and low-latitude regions around the world has shown a decreasing trend [2–4]. Chinese scholars also indicate a significant decreasing trend in the annual average wind

speed in China [5–7]. For example, REN, et al. [8] found that in the past 47 years, the annual average wind speed in China has decreased by over $0.01 \text{ m}\cdot\text{s}^{-1}$. XU, et al. [9] pointed out that from 1969 to 2000, the annual average wind speed in China steadily decreased by 28%, and the days with a daily average wind speed greater than $5 \text{ m}\cdot\text{s}^{-1}$ decreased by 58%.

For regional extreme wind and precipitation events, some studies [10] show that typhoons and gales rapidly decrease from coastal provinces to inland areas in China, and coastal areas (especially coastal areas of East and South China) have the maximum value of annual average days of typhoon extreme wind. The analysis results from 1961 to 2001 indicate that both the average precipitation and frequency of extreme precipitation events in the Yangtze River Basin have been on the rise, with summer extreme precipitation events sharply increasing at a rate of 10% to 20% every 10 years [11].

The compound extreme events have received attention in recent years [12], and researchers point out that their catastrophic effects are often stronger than single extreme events [13,14]. This article focuses on how compound extreme precipitation events and extreme wind events (hereinafter referred to as compound extreme wind and precipitation events) will change as extreme precipitation events become more frequent and average wind speeds decrease significantly. The Jiangsu–Anhui region is located in the subtropical monsoon region, adjacent to the Yellow Sea and Yangtze River basins in China. It has abundant rainfall, luxuriant vegetation, and high population aggregation. At the same time, the Jiangsu–Anhui region is one of the regions where rainstorms, floods, gales, and other disasters occur most seriously in China. Therefore, focusing on the compound extreme wind and precipitation events in this region can provide a reference for the diagnosis and prediction of disastrous weather.

2. Data and Methods

2.1. Data

The research period in this paper is from spring in 1961 to spring in 2020 (March to May), and the data used in the paper are as follows:

1. The daily precipitation and wind speed observation data from stations are provided by the Information Center of the China Meteorological Administration. After removing the stations with missing data, a total of 125 stations remained, and their distribution is shown in Figure 1.
2. The monthly average reanalysis data is from the National Centers for Environmental Prediction (NCEP) and the National Center for Atmospheric Research (NCAR), and the elements used are geopotential height field, wind field, precipitable water, and vertical velocity, with a horizontal resolution of $2.5^\circ \times 2.5^\circ$.

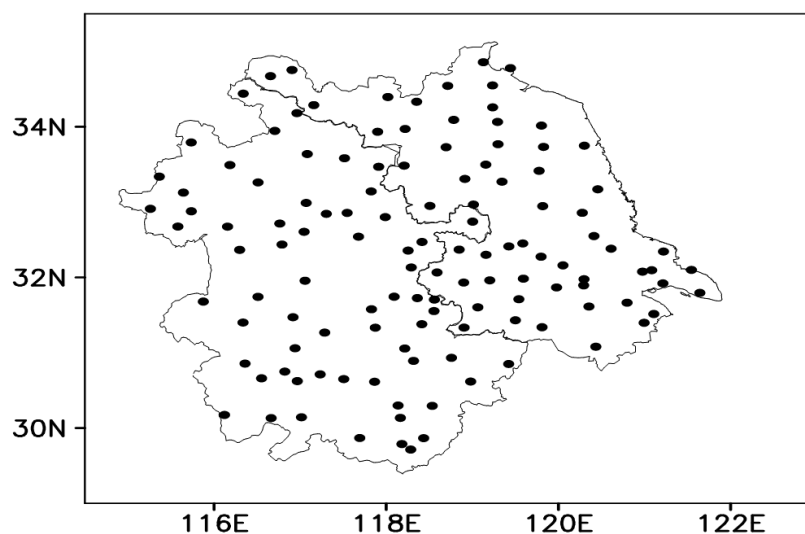


Figure 1. Spatial distribution of 125 weather stations across the Jiangsu–Anhui region.

2.2. Definition of the Compound Extreme Wind and Precipitation Events

Compound extreme events can be combinations of temporal, spatial, or spatiotemporal extreme events. This paper adopts a spatiotemporal compound method to define compound extreme wind and precipitation events [15] and also adopts a percentile threshold to define a single extreme event. Specifically, the average wind speed or precipitation on the same day at a certain station from 1991 to 2020 (climatic standard period) would be arranged in ascending order, and the 90th percentile value would be selected as the threshold for an extreme wind or precipitation event in order to obtain the extreme wind or precipitation threshold for each day in a spring of 92 days. When the average wind speed and precipitation at a certain station on a certain day are either greater than or equal to the threshold of the day, it is determined as a compound extreme wind and precipitation event, recorded as CWPE (Composite Wind and Precipitation Extreme).

2.3. Hodrick–Prescott Filtering Method

The Hodrick–Prescott (HP) filtering method is used for time series analysis in this paper. This method can eliminate the trend components contained in the time series and effectively capture the characteristics of data fluctuations [16]. Based on the principle of time series spectral analysis, the time series of compound extreme wind and precipitation events are regarded as the superposition of components with different frequencies. Through high-pass filtering, the interdecadal fluctuations (high-frequency components) and long-term trends (low-frequency components) are separated. The low-frequency components are obtained by the following minimization Formula (1):

$$\min \left\{ \sum_{t=1}^n (y_t - g_t)^2 + \lambda (c(I)g_t) \right\} \quad (1)$$

In Equation (1), $c(I)$ is the backshift operator polynomial, whose formula is as follows:

$$c(I) = (I^{-1} - 1) - (1 - I) \quad (2)$$

In Equation (2), I is the retardation factor, fixed and given by the econometric model. By introducing Equation (2) into Equation (1), the solution for the minimizing function is as follows:

$$\min \left\{ \sum_{t=1}^n (y_t - g_t)^2 + \lambda \sum_{t=2}^n [(g_{t+1} - g_t) - (g_t - g_{t-1})]^2 \right\} \quad (3)$$

In Equation (3), λ is the HP filtering parameter. When $\lambda = 0$, the solution for the minimizing function is the $\{y_t\}$ sequence. As the λ value increases, the trend of the minimizing estimation becomes smoother. The empirical parameters of λ are 100 for annual data, 1600 for quarterly data, and 14,400 for monthly data. In this paper, the λ value is 100.

3. Results and Analysis

3.1. Spatial Distribution Characteristics

Firstly, this paper understands the climatic characteristics of the CWPE in Jiangsu and Anhui Provinces. Figure 2 shows the frequency distribution of the CWPE in spring over the Jiangsu–Anhui region from 1961 to 2020. It is not difficult to find that in the past 60 years, the CWPE in the Jiangsu–Anhui region has presented a distribution pattern of less in the south and more in the north. The frequency is the highest in the northern region of Jiangsu, with some stations exceeding four days. The frequency is relatively low in the southern region of Anhui, with a minimum of less than two days.

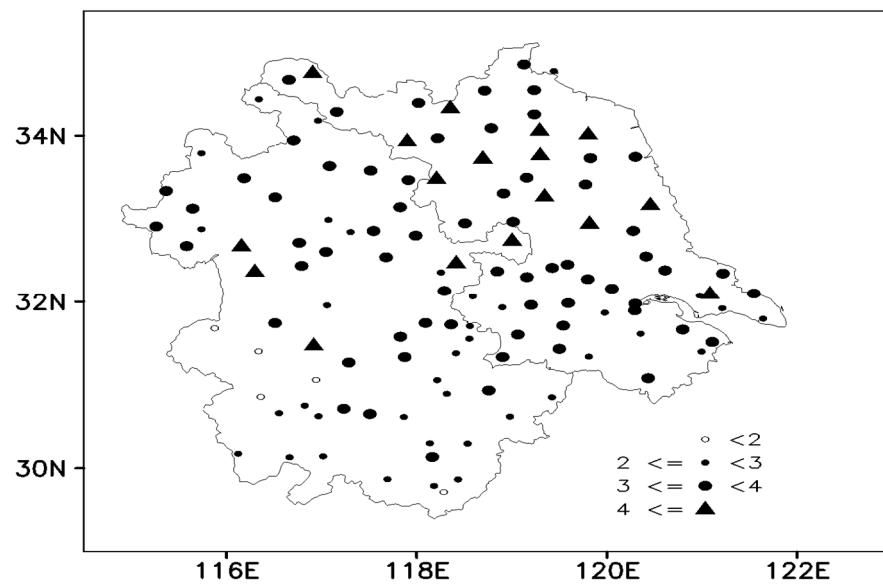


Figure 2. Spatial distribution of CWPE frequency in spring over the Jiangsu–Anhui region (unit: d).

As shown in Figure 3, it can be seen that from 1961 to 2020, the spring CWPE over the Jiangsu–Anhui region has shown a consistent downward trend throughout the region, and the region with the highest frequency of CWPE had the most significant decline. The decrease in the CWPE in northern Jiangsu is as high as 1–2 d/10 a, while in southern Jiangsu and central-northern Anhui, it is between 0.5 and 1 d/10 a. The decrease in the CWPE in southern Anhui is the smallest, basically less than 0.5 d/10 a. Except for Tongcheng station in Anhui Province, the spring CWPE climatic tendency rates of other stations in the region have all passed the 95% confidence test, which indicates that the spring CWPE in the Jiangsu–Anhui region over the past 60 years has a significant downward trend.

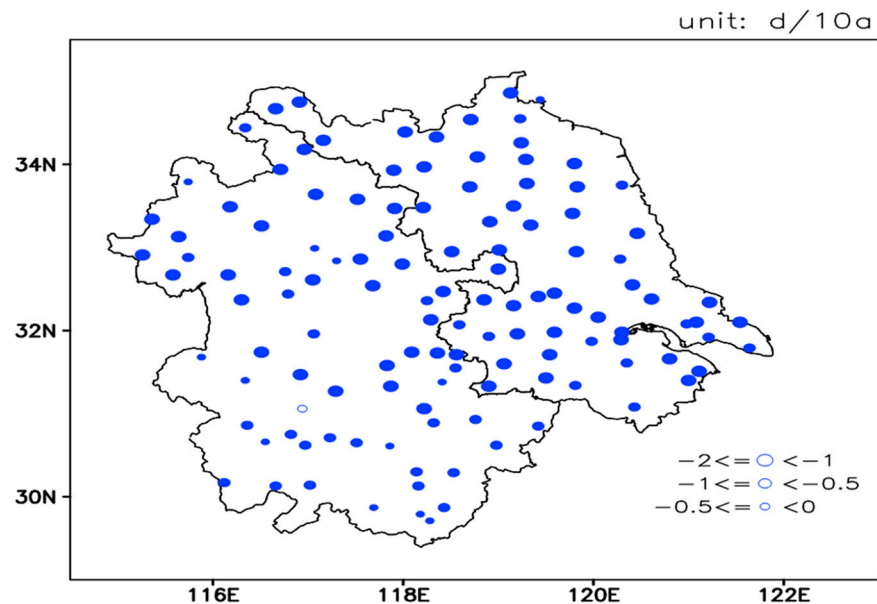


Figure 3. CWPE climatic tendency rate in spring during 1961 to 2020 (unit: d/10 a, solid dots indicate passing 95% confidence test).

3.2. Temporal Distribution Characteristics

Figure 4 shows the interannual variation of average spring CWPE in the Jiangsu–Anhui region. Consistent with the analysis of climatic variability in the previous text, the frequency of the CWPE in spring has presented a significant downward trend in the past

60 years, with a rate of 0.1 d/a. After the 1990s, the frequency was relatively low, with the lowest frequency in 2001 and an average annual occurrence of less than one day. Moreover, the decreasing trend gradually slows down after the 1990s.

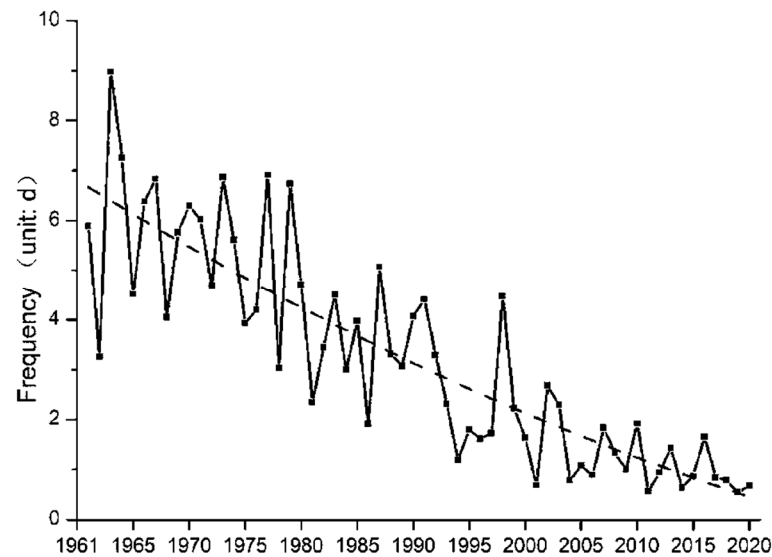


Figure 4. The interannual changes of spring CWPE in the Jiangsu–Anhui region from 1961 to 2020 (unit: d).

In order to analyze the periodic characteristics of spring CWPE in the Jiangsu–Anhui region, the wavelet analysis was performed on the CWPE, shown in Figure 5. CWPE has a significant quasi-3-year interannual oscillation period, mainly occurring between 1965 and 1980 and around 1990. Before 1990, there was an interannual oscillation period of 2–4 years in the spring CWPE of the Jiangsu–Anhui region, and the period from 1960 to 1980 was more obvious.

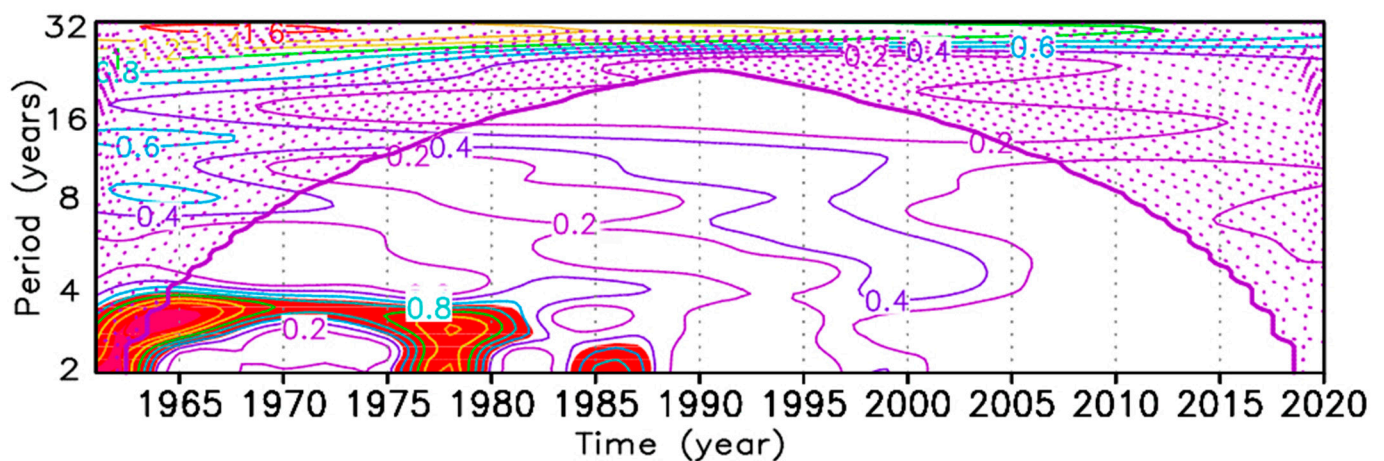


Figure 5. The wavelet power spectrum of CWPE in spring of the Jiangsu–Anhui region from 1961 to 2020.

In order to further obtain the spatiotemporal variation characteristics of the CWPE, EOF decomposition was conducted on the CWPE in spring over the Jiangsu–Anhui region from 1961 to 2020. Table 1 shows the variance contribution rate of the first five modal eigenvalues of CWPE and their corresponding cumulative variance contribution rate. The variance contribution rate of the first mode is more than 60% and has passed the North test, which indicates that the first mode of EOF of the CWPE in spring over the Jiangsu–Anhui region contains sufficient effective information and can typically reflect

the main temporal and spatial distribution characteristics of the CWPE in spring over the Jiangsu–Anhui region.

Table 1. Variance contribution rate of the first five modal eigenvalues of CWPE and their corresponding cumulative variance contribution rate in spring over Jiangsu–Anhui region.

EOF Variance Contribution	First Mode	Second Mode	Third Mode	Fourth Mode	Fifth Mode
Spring					
Variance contribution	60.66% *	5% *	3.07% *	2.76% *	2.37% *
Accumulated contribution	60.66%	65.66%	68.73%	71.49%	73.86%

Note: Marked with “*” indicates passing the North test.

It can be seen from Figure 6a that the spatial distribution of the first mode of EOF of the CWPE in spring over the Jiangsu–Anhui region is consistently distributed throughout the region. There exists a high value area near Tongling, Anhui, with the variance contribution of the first mode reaching 60.66%, which indicates that the overall region presents a consistent variation trend in spring. From the perspective of the evolution curve of the time coefficient of the first characteristic vector and its linear trend, the CWPE in spring presents an obvious downward trend (Figure 6b). After the 1990s, the EOF1 time coefficient of the CWPE frequency in the Jiangsu–Anhui regions was mostly negative in most years. Combined with spatial patterns, it is indicated that the CWPE frequency during this period was low and negative anomalies appeared, which is consistent with previous interannual change analyses.

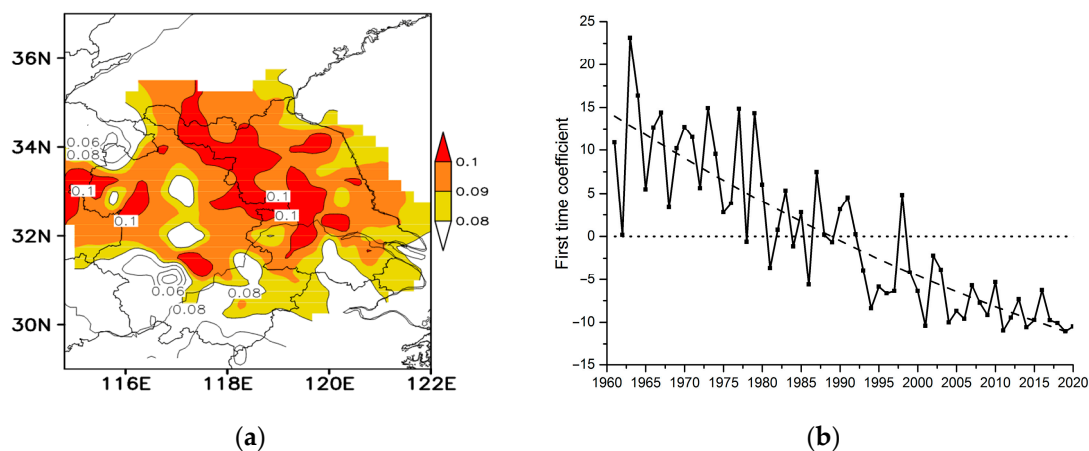


Figure 6. (a) The first mode of EOF of CWPE in spring over the Jiangsu–Anhui region and (b) its corresponding time coefficient.

According to the trend analysis of CWPE frequency and EOF decomposition, there has been a significant decreasing trend of CWPE in spring over the Jiangsu–Anhui region in the past 60 years. The results of the MK mutation test also confirmed the interdecadal transition in the CWPE frequency in spring over the Jiangsu–Anhui region during the 1990s (Figure 7). According to the UF curve, CWPE frequency has shown a significant decrease since the 1980s. Based on the intersection position of the UF and UB curves, it can be preliminarily seen that there may be an interdecadal transition of the CWPE in spring in the early 1990s.

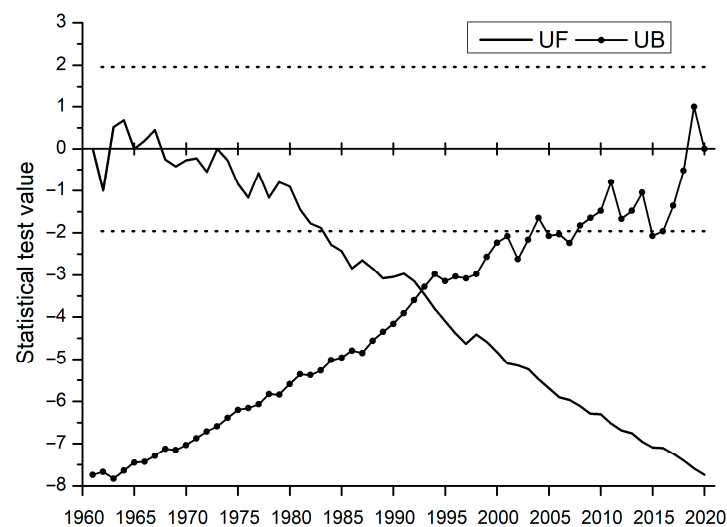


Figure 7. Mann-Kendall statistics of CWPE events in spring during 1961 to 2020.

3.3. Circulation Background of Interannual Anomalies

According to the previous analysis, there are significant interdecadal differences in the CWPE between Jiangsu and Anhui Provinces. Therefore, the HP filtering method can be used to remove interdecadal variation interference after filtering. Figure 8 shows the time series of the CWPE frequency in spring over the Jiangsu–Anhui region after HP filtering. It can be seen that there exists a significant interannual anomaly in the CWPE frequency in spring, and the oscillation amplitude of the interannual anomaly has presented an obvious decreasing trend in the past 60 years. Before the 1990s, the amplitude of the CWPE in spring was relatively large. After filtering, it was found that the spring in 1963 had the highest CWPE frequency, while 1962 had the lowest. Then, the circulation of the CWPE in spring in high-frequency and low-frequency years was comparatively analyzed. Firstly, the filtered time series was conducted standardize the anomaly, and then the three years with the highest absolute value were selected as the years with abnormally high (including 1963, 1979, and 1998) and abnormally low (including 1962, 1968, and 1981) values.

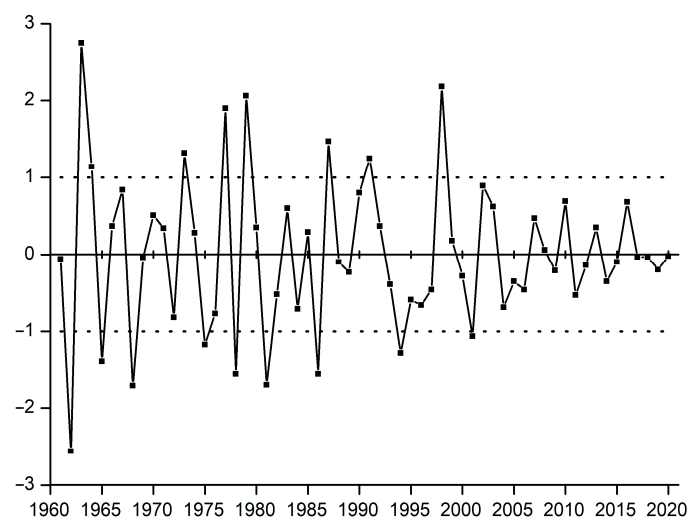


Figure 8. The time series of the CWPE frequency in spring over the Jiangsu–Anhui region after HP filtering during 1961 to 2020.

From the perspective of the spatial distribution of the 200 hPa height field anomalies in high-frequency and low-frequency years (Figure 9), it can be seen that a clear positive anomaly center exists in the Lake Baikal area, while a negative anomaly center exists at the

junction of China, India, and Pakistan in Eurasia. The spatial distribution of the 500 hPa height field anomaly (Figure 10) also shows that, in high-frequency years, the anomaly of north of 45° N is positive, while the south of 45° N is negative. Under this kind of circulation background, it is conducive to enhance the high-latitude high pressure, increase the meridional gradient of circulation, and thus promote the activity of high-latitude short-wave trough ridges, which make cold air activity frequent. Active cold air can be beneficial to precipitation. In addition, the continuous southward movement of cold air is conducive to the increase in strong winds, which make CWPEs more prone to occur. Overall, there is a significant difference between the anomaly at the 200 hPa and 500 hPa height fields in low-frequency years and in high-frequency years. In low-frequency years, the synthetic height anomaly field in the middle and high latitudes presents a consistent negative anomaly, especially in the vicinity of 30° N where the Jiangsu–Anhui region is located with a high-value negative anomaly. The center values of 200 hPa and 500 hPa can reach -330 dagpm and -200 dagpm, respectively. In this case, the high pressure in high latitude areas weakens, and the meridional gradient of the circulation decreases, which is not conducive to the southward movement of cold air. Correspondingly, it is difficult for cold and warm airflow to converge in the Jiangsu–Anhui region, and the frequency of precipitation and strong wind events decreases, leading to a decrease in the occurrence of compound extreme wind and precipitation events.

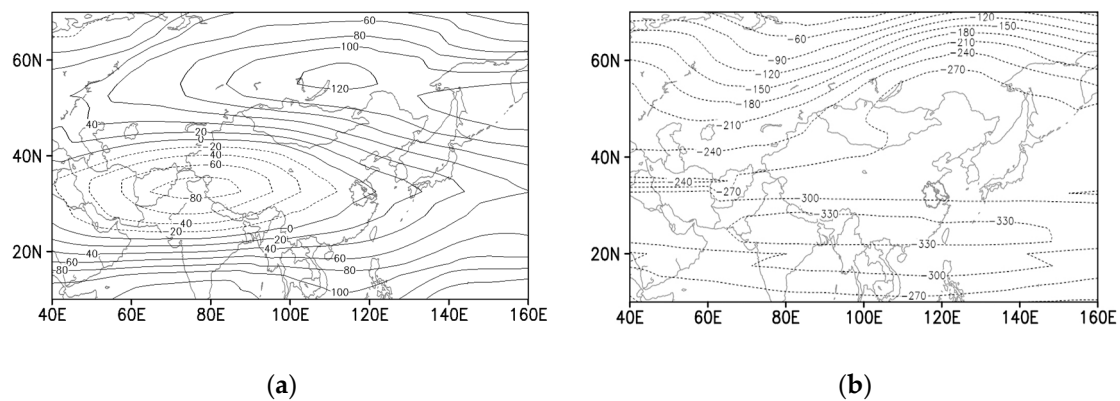


Figure 9. Distribution of 200 hPa geopotential height field anomalies corresponding to high-frequency (a) and low-frequency (b) years of CWPE in spring over the Jiangsu–Anhui region.

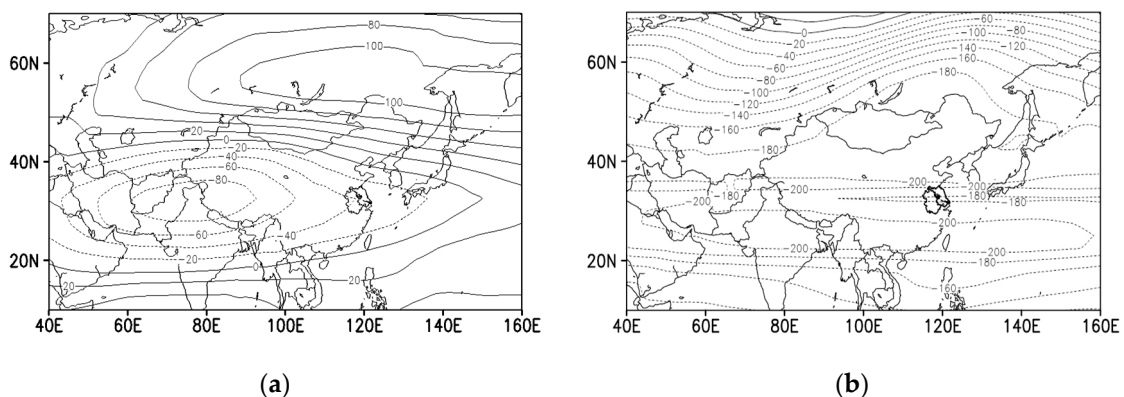


Figure 10. Distribution of 500 hPa geopotential height field anomalies corresponding to high-frequency (a) and low-frequency (b) years of CWPE in spring over the Jiangsu–Anhui region.

Further analysis of wind field anomaly in high-frequency and low-frequency years shows that there exists a cyclonic anomalous shear in the 500 hPa wind field near Nepal and Taiwan Island, China, in high-frequency years, while a consistent east to southeast wind anomaly exists in the Jiangsu–Anhui region (Figure 11). At the 850 hPa wind field,

a strong southwest air flow travels from the Bay of Bengal to the Jiangsu–Anhui region in the middle and low latitudes (Figure 12). In addition, the air flow in the East China Sea also continues to travel to the regions. Abundant water vapor converges with cold air southward in the high latitudes, which is conducive to the increase in precipitation, so the extreme precipitation events are more likely to occur. In low-frequency years, the wind fields at 500 hPa and 850 hPa are dominated by easterly anomaly advection in most areas south of 40° N, while there is no effective water vapor transportation belt in the middle and low latitudes, and the water vapor transportation belt from the Bay of Bengal to the Jiangsu–Anhui regions is weak, so the water vapor transportation conditions are poor. In addition, from the 500 hPa circulation field, it can be observed that in low-frequency years, the meridional gradient in the middle and high latitudes in spring is relatively small, and the cold air is not active, making it difficult to form heavier precipitation. The frequency of the compound extreme wind and precipitation events is relatively low.

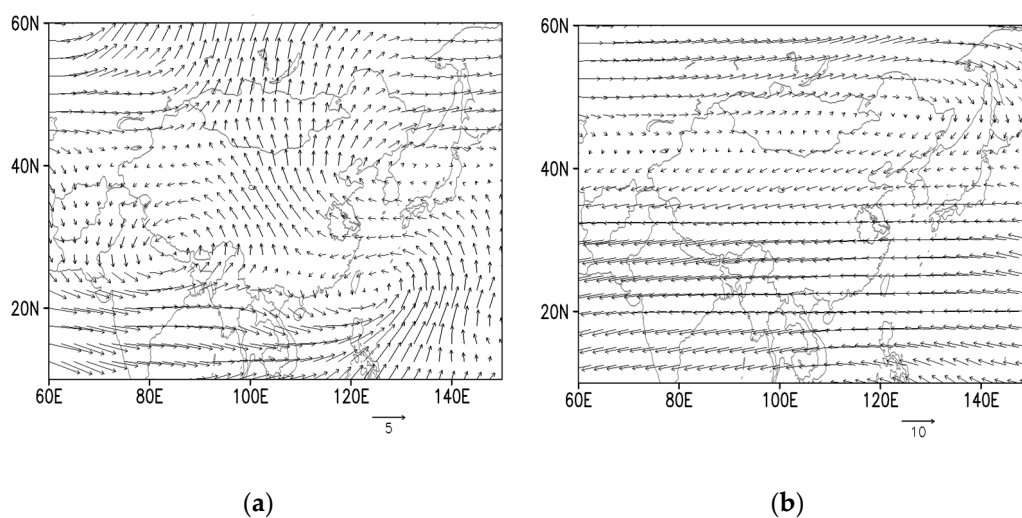


Figure 11. Anomalous distribution of 500 hPa wind field of CWPE in spring over the Jiangsu–Anhui regions in high-frequency (a) and low-frequency (b) years (unit: $\text{m}\cdot\text{s}^{-1}$).

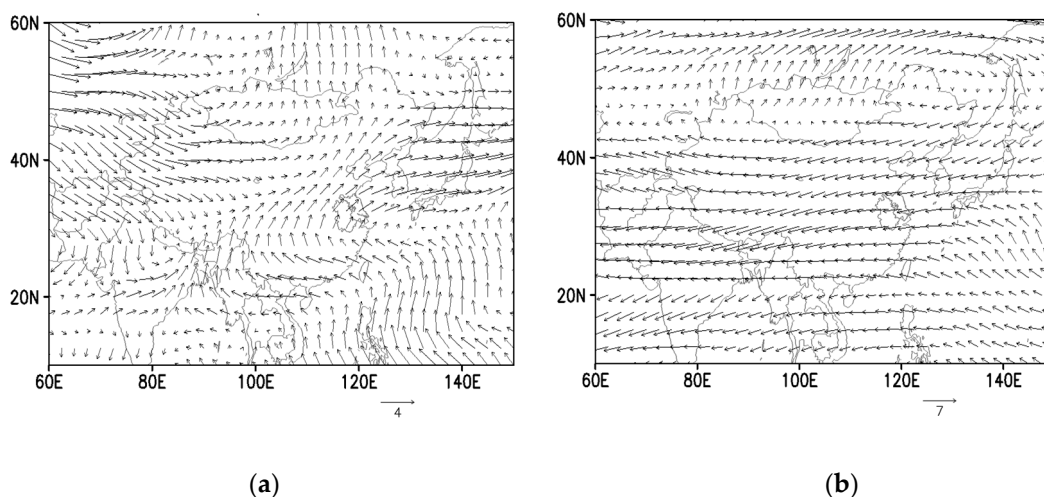


Figure 12. Anomalous distribution of 850 hPa wind field of CWPE in spring over the Jiangsu–Anhui region in high-frequency (a) and low-frequency (b) years (unit: $\text{m}\cdot\text{s}^{-1}$).

From the perspective of precipitable water (Figure 13), it can be seen that the precipitable water of the CWPE in spring over the Jiangsu–Anhui region in high-frequency years is significantly higher than the climatic average. The precipitable water in high-frequency years over the Jiangsu–Anhui region is the high value center, which is basically $3\text{--}4 \text{ kg}\cdot\text{m}^{-2}$

higher than the climatic average. This indicates that during the high-frequency years, the water vapor content over the Jiangsu–Anhui regions is higher, which is conducive to the increase in extreme precipitation events. On the contrary, during the low-frequency years, the precipitable water in the Jiangsu–Anhui region is significantly lower than the climatic average field. The precipitable water in the northern part of the Jiangsu–Anhui region decreases most significantly, which is basically $5\text{--}7\text{ kg}\cdot\text{m}^{-2}$ lower than the climatic average, while the precipitable water in southern part of the Jiangsu–Anhui region decreases by $3\text{--}4\text{ kg}\cdot\text{m}^{-2}$. Therefore, the water vapor content in the northern part of the Jiangsu–Anhui region is severely insufficient, which is not conducive to the precipitation and the corresponding compound extreme events.

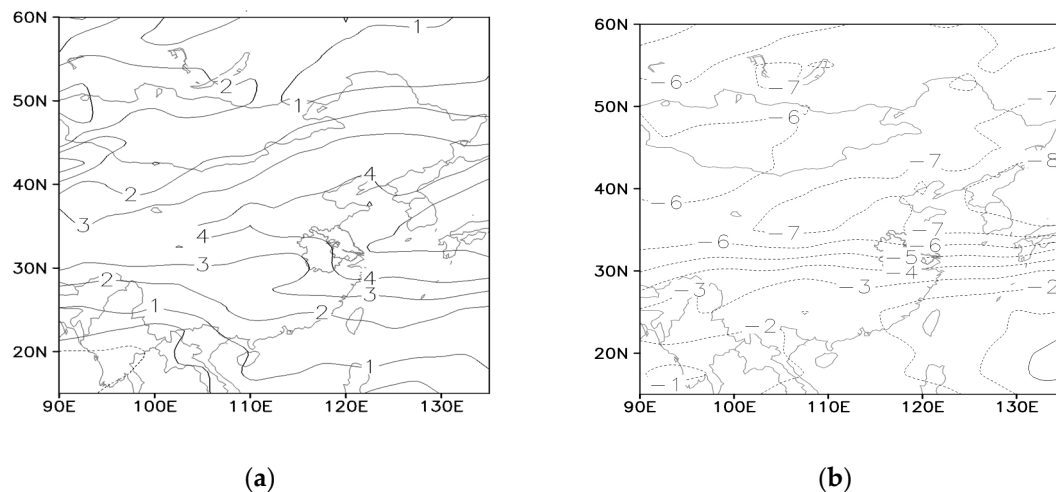


Figure 13. Anomalous distribution of precipitable water of CWPE in spring over the Jiangsu–Anhui region in high-frequency (a) and low-frequency (b) years (unit: $\text{kg}\cdot\text{m}^{-2}$).

The vertical velocity field often reflects the activity of convective motion, and the stronger the precipitation, the greater the vertical velocity. From Figure 14, it can be seen that in high-frequency years, the vertical velocity over the Jiangsu–Anhui region is relatively high, which is $0.015\text{ Pa}\cdot\text{s}^{-1}$ higher than the climatic average. At this time, the convection development is more exuberant, which also reveals that in years with more compound wind and precipitation events, more extreme precipitation occurs, and convective motion is also more exuberant than the climatic state. Strong convective motion can not only bring extreme precipitation but can also cause local thunderstorms and gales, making compound extreme wind and precipitation events easier to occur. The low-frequency years are the opposite. The vertical velocity over the northern part of the Jiangsu–Anhui region is a positive anomaly center, which is $0.01\text{ Pa}\cdot\text{s}^{-1}$ less than the climatic average. At this time, the convective motion is weak, which is closely related to the difficulty of cold air moving southward from the north and the lack of water vapor transportation. In addition, the weak convective motion also makes it difficult to form thunderstorm and gale weather. Therefore, there exists a significant difference in the vertical velocity field between years with high-frequency and low-frequency CWPE events in spring.

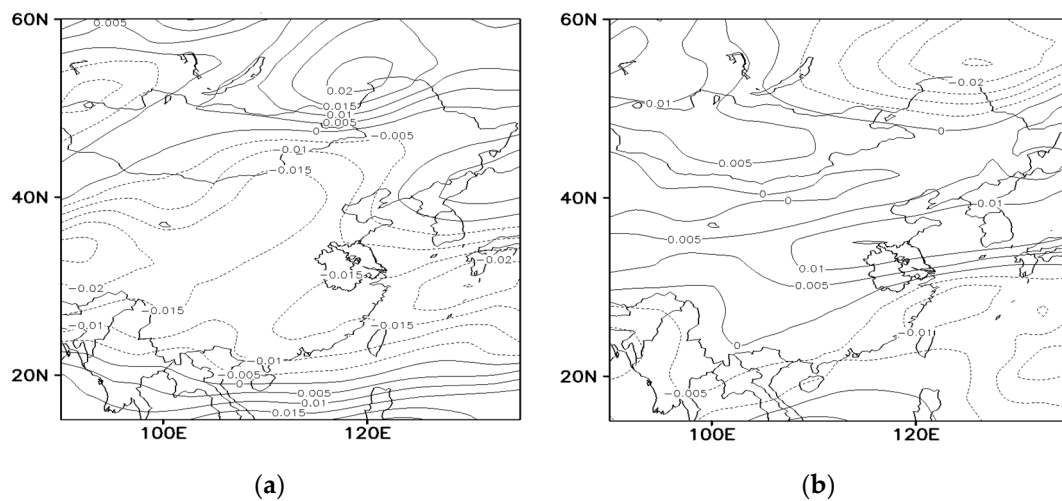


Figure 14. Anomalous distribution of vertical velocity of CWPE in spring over the Jiangsu–Anhui region in high-frequency (a) and low-frequency (b) years (unit: $\text{Pa}\cdot\text{s}^{-1}$).

4. Conclusions

By using the daily wind speed and precipitation data from 125 stations in the Jiangsu–Anhui region of China from 1961 to 2020, as well as NCEP/NCAR reanalysis data, the variation characteristics of spring compound extreme wind and precipitation events in the Jiangsu–Anhui region were analyzed, and the circulation background of their interannual anomalies were explored. The conclusions are as follows:

1. The spring compound extreme wind and precipitation events in the Jiangsu–Anhui region presents a distribution pattern of less in the south and more in the north. Stations south of 32°N are mostly below three days, while stations north of 32°N are mostly above three days; moreover, some stations in northern Jiangsu are over four days.
2. The frequency of spring compound extreme wind and precipitation events experienced an interdecadal mutation from more to less in the early 1990s. This kind of interdecadal variation covered the entire Jiangsu–Anhui region, and the decrease was more significant in the coastal area of northern Jiangsu with the highest frequency.
3. The characteristics of the compound height anomaly field at 200 hPa and 500 hPa in high-frequency years are the following: north of 45°N is a positive anomaly while south of 45°N is a negative anomaly. This circulation background enhances the high pressure in high latitudes and increases the meridional direction of the circulation, which is conducive to the activity of high-latitude short-wave trough ridges and frequent cold air activity. Corresponding to 850 hPa in the middle and low latitudes, a strong southwest air flow travels from the Bay of Bengal to the Jiangsu–Anhui region. The convergence of abundant water vapor with southward cold air in high latitudes is conducive to the occurrence of extreme events. At the same time, the precipitable water in the Jiangsu–Anhui region is located at the center of the high anomaly value, corresponding to a larger vertical velocity above the sky and a stronger convective development, which promotes the occurrence of compound extreme wind and precipitation events more easily.
4. In the low-frequency years, a consistent negative anomaly is presented in the middle- and high-latitude regions, especially in the vicinity of the Jiangsu–Anhui region with a high-value area for the negative anomaly, which weakens the high pressure in the high-latitude regions and reduces the meridional circulation degree, so it is not conducive to the southward movement of cold air. It is difficult for cold and warm airflow to converge in the Jiangsu–Anhui region. The reduction in the frequency of precipitation and the corresponding gale events leads to a decrease in compound extreme wind and precipitation events. Most areas south of 40°N

at 500 hPa and 850 hPa are dominated by easterly anomaly advection. There is no effective water vapor transportation belt in the middle and low latitudes. The water vapor transportation belt from the Bay of Bengal to the Jiangsu–Anhui region is weak, so the water vapor transportation conditions are poor. The precipitable water in the Jiangsu–Anhui region is significantly less than the average climatic field. The vertical velocity over the northern part of the Jiangsu–Anhui region is the center of a positive anomaly, and the weak convective motion is not conducive to precipitation; moreover, it is also difficult to form thunderstorms and gale weather, and the corresponding compound extreme events decrease relatively.

Research on compound extreme wind and precipitation events in the Jiangsu–Anhui region is still rare. This study explores the interannual anomalies and circulation background of spring compound extreme wind and precipitation events in the region for the first time, which provides useful references for the diagnosis and prediction of catastrophic weather in the region. The influence mechanism of compound extreme events is relatively complex. According to the research, there was an obvious interdecadal transition in early 1990, considering that the urbanization process in the Jiangsu–Anhui region has accelerated since the 1990s. By changing the characteristics of the underlying surface, the urbanization changes the structure of the atmospheric boundary layer and the balance of surface energy and other dynamic processes, so as to affect regional climate significantly. Subsequent research can analyze the causes of interdecadal variation in the CWPE in the Jiangsu–Anhui region from the perspective of urbanization.

Author Contributions: Conceptualization, J.Z.; methodology, J.Z. and Y.S.; software, L.L.; formal analysis, J.Z.; investigation, J.Z.; data curation, L.Z.; writing—original draft preparation, J.Z.; writing—review and editing, Y.S. All authors have read and agreed to the published version of the manuscript.

Funding: This research was funded by the National Natural Science Foundation of China under grant 41575010.

Institutional Review Board Statement: Not applicable.

Informed Consent Statement: Not applicable.

Data Availability Statement: Not applicable.

Conflicts of Interest: The authors declare no conflict of interest.

References

1. IPCC. *Climate Change 2021: The Physical Science Basis*; Cambridge University Press: Cambridge, UK, 2021.
2. Smits, A.; Tank, A.; Knnen, G.P. *Trends in Storminess over the Netherlands, 1962–2002*; John Wiley & Sons, Ltd.: Hoboken, NJ, USA, 2005; Volume 10.
3. Pryor, S.C.; Barthelmie, R.J.; Riley, E.S. Historical evolution of wind climates in the USA. *J. Phys. Conf. Ser.* **2007**, *75*, 012065.
4. McVicar, T.R.; Van Niel, T.G.; Li, L.T.; Roderick, M.L.; Rayner, D.P.; Ricciardulli, L.; Donohue, R.J. Wind speed climatology and trends for Australia, 1975–2006. *Geophys. Res. Lett.* **2008**, *35*, L20403.
5. Wang, Z.; Ding, Y.; He, J.; Yu, J. An updating analysis of the climate change in China in recent 50 years. *Acta Meteorol. Sin.* **2004**, *62*, 228–236. (In Chinese)
6. Wang, X.; Zhai, P. The spatial and temporal variations of spring dust storms in China and its associations with surface winds and sea level pressures. *Acta Meteorol. Sin.* **2004**, *62*, 96–103. (In Chinese)
7. Jiang, Y.; Luo, Y.; Zhao, Z.; Tao, S. Changes in wind speed over China during 1956–2004. *Theor. Appl. Climatol.* **2010**, *99*, 421–430.
8. Ren, G.; Guo, J.; Xu, M.; Chu, Z.; Zhang, L.; Zou, X.; Li, Q.; Liu, X. Climate changes of China’s mainland over the past half century. *Acta Meteorol. Sin.* **2005**, *63*, 94–956. (In Chinese)
9. Xu, M.; Chang, C.P.; Fu, C.; Qi, Y.; Robock, A.; Robinson, D.; Zhang, H.M. Steady decline of East Asian monsoon winds, 1969–2000: Evidence from direct ground measurements of wind speed. *J. Geophys. Res.* **2006**, *111*, 1–8. [[CrossRef](#)]
10. Yi, L.; Weijun, Z.; Fumin, R.; Xin, W. Changes of tropical cyclone high winds and extreme winds during 1980–2014 over China. *Clim. Chang. Res.* **2016**, *12*, 413–421. (In Chinese)
11. Wang, Y.; Zhou, L. Observed trends in extreme precipitation events in China during 1961–2001 and the associated changes in large-scale circulation. *Geophys. Res. Lett.* **2005**, *32*, L09707. [[CrossRef](#)]
12. IPCC. *Summary for Policymaker*; Cambridge University Press: Cambridge, UK, 2021.

13. Leonard, M.; Westra, S.; Phatak, A.; Lambert, M.; van den Hurk, B.; McInnes, K.; Risbey, J.; Schuster, S.; Jakob, D.; Stafford-Smith, M. A compound event framework for understanding extreme impacts. *Wiley Interdiscip. Rev. Clim. Chang.* **2014**, *5*, 113–128. [[CrossRef](#)]
14. McPhillips, L.E.; Chang, H.; Chester, M.V.; Depietri, Y.; Friedman, E.; Grimm, N.B.; Kominoski, J.S.; McPhearson, T.; Méndez-Lázaro, P.; Rosi, E.J.; et al. Defining extreme events: A cross-disciplinary review. *Earth's Future* **2018**, *6*, 441–455. [[CrossRef](#)]
15. Yu, R.; Zhai, P. Advances in scientific understanding on compound extreme events. *Trans. Atmos. Sci.* **2021**, *44*, 645–649. (In Chinese) [[CrossRef](#)]
16. Hodrick, R.J.; Edward, C.P. Postwar US business cycles: An empirical investigation. *J. Money Credit Bank.* **1997**, *29*, 1–16. [[CrossRef](#)]

Disclaimer/Publisher's Note: The statements, opinions and data contained in all publications are solely those of the individual author(s) and contributor(s) and not of MDPI and/or the editor(s). MDPI and/or the editor(s) disclaim responsibility for any injury to people or property resulting from any ideas, methods, instructions or products referred to in the content.